Available online at www.sciencedirect.com
SCIENCE DIRECT®
International Journal of Heat and Mass Transfer 49 (2006) 1845–1850
International Journal of HEAT and MASS TRANSFER
www.elsevier.com/locate/ijhmt

Thermodynamic formulation of temperature–entropy diagram for the transient operation of a pulsed thermoelectric cooler

Anutosh Chakraborty, Kim Choon Ng *

Mechanical Engineering Department, National University of Singapore, 10 Kent Ridge Crescent, Singapore 119260, Singapore

Received 25 April 2005
Available online 9 January 2006

Abstract

A general thermodynamic formulation for the operation of a pulsed thermoelectric cooler is presented using the Gibbs law and simple energy balance method. An expression for the entropy flux (W/m^2 K) is expressed in terms of the key parameters employed for the thermoelectric operation. Following the classical temperature–entropy (T–s) methodology, which has all the virtues of energy flow identification, the processes along the p–n legs of thermoelectrics, contributing to both useful and dissipative losses, are clearly mapped for the transient operation.

Keywords: Thermoelectrics; T–s diagram; Pulsed thermoelectrics; Entropy flux

1. Introduction

In 1958, the transient behaviours of a thermoelectric cooler that comprised two thermoelectric elements was first reported by Stil'bans and Fedorovitch [1] where they soldered two thermoelectric elements together to for the purpose of reducing the thermal mass at fast operation. Then in 1961, Landecker and Findlay [2] studied extensively the transient behaviour of Peltier junctions by devising a method for measuring the thermo-junction temperature after the passage of transient current pulse. They have theoretically demonstrated that the cold junction temporal profile is a function of both pulse current and duration. Experimental studies with high current pulse and finite cold junction were carried out by Field and Blum [3] and they provided the quantitative data for the pulse cooling mode for the coolers with a finite cold surface mass and contact resistance.

In 2002, Snyder et al. [4] reported the possibility of having a super-cooler that employs a Peltier device and exploiting the short time scale behaviour of the current pulse at a magnitude of several folds higher than that of the non-pulsing period. The Peltier cold junction breaks contact momentarily with the surface to be cooled prior to the arrival of the Joulean heat, where the latter is a heat transfer phenomenon with a slower time-scale. Such a transient operation of the thermoelectrics has enabled these cooling devices to reach an unprecedented low temperature level, typically about 220–240 K which widens the application potential of pulsed thermoelectrics, for example, a cryo-cooler for surgery applications or the cooling of infrared detectors.

In this paper, the authors focus on the theoretical modeling of the pulsed thermoelectrics using the classical thermodynamic framework of the Gibbs law. Following such an approach and using only the key parameters of the Peltier device, they are able to formulate the governing equations for tracking the paths of thermal processes using a temperature–entropy flux diagram so as to capture accurately the device's useful and dissipative energy or losses at transients. Such a thermodynamic approach will depict succinctly the energy flow and dissipative "bottlenecks" along the p–n legs of thermoelectrics and demonstrates

* Corresponding author. Tel.: +65 68742214; fax: +65 67791459.
E-mail address: mpengkc@nus.edu.sg (K.C. Ng).

0017-9310/$ - see front matter © 2005 Elsevier Ltd. All rights reserved.
doi:10.1016/j.ijheatmasstransfer.2005.10.038

Nomenclature

A	cross-section area (m^2)
c_p	specific heat capacity (J/kg K)
h	enthalpy per unit mass (J/kg)
I	current (A)
$\mathbf{J}$	current density (A/m^2)
$\mathbf{J}_S$	entropy flux (W/m^2 K)
L	thermoelectric length
p	the pressure of the system (Pa)
$\dot{q}$	heat flux (W/m^2)
$\mathbf{S}_{gen}$	entropy generation (W/m^3 K)
s	entropy (J/kg K)
T	temperature (K)
t	time (s)
u	internal energy per unit mass (J/kg)
v	specific volume (m^3/kg)
x	co-ordinate across X-axis (m)
α	Seebeck coefficient (V/K)
ρ	density (kg/m^3)
σ	electrical conductivity (1/ohm m)
λ	thermal conductivity (W/m K)
π	Peltier coefficient (V)
Γ	Thomson coefficient (V/K)

Subscripts

cj	cold junction
gen	generation
hj	hot junction
max	maximum
np	non-pulse
p	pulse
subs	substrates

the pedagogical value of T–s diagram of the device during transients, as opposed to the T–s diagrams for steady state cycles [5].

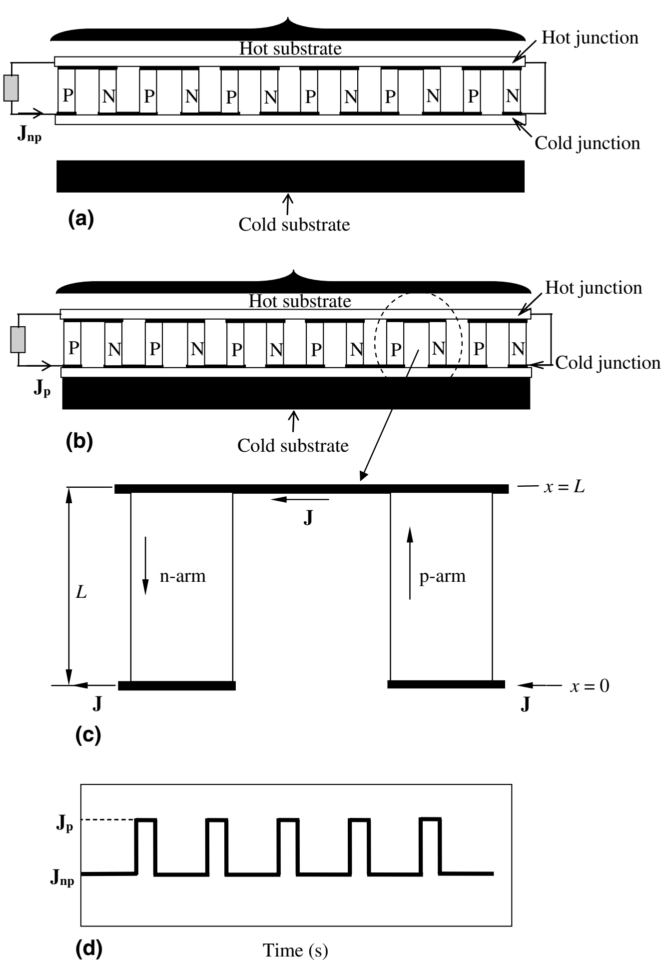

Fig. 1. Schematic diagram of the first transient thermoelectric cooler.

Fig. 1(a)–(d) shows the schematic diagrams of a typical pulsed thermoelectric cooler with the p- and n-doped semiconductor elements or legs which are electrically connected in series but thermally in parallel: In Fig. 1(a) and (b), the elements shown are in the contact and non-contact modes of operation. The hot side of the device is mounted directly onto a substrate where heat can be rejected to the environment whilst the cold junction makes contact in a periodical manner, during which the cold substrate is cooled. Fig. 1(c) shows the schematic representation of the thermoelectric couple. The typical current pulses are shown in Fig. 1(d), depicting the ''open'' and ''close'' periods. Current flowing into the elements is made to pulse between $\mathbf{J}_{np}$ and $\mathbf{J}_p$: $\mathbf{J}_p$ can be of several orders higher than $\mathbf{J}_{np}$, giving intense Peltier cooling during contact due to the small time-scale phenomenon of energy being carried away by the electrons and holes, and hence achieves the desired cooling. The time duration of the pulse is therefore dictated by the presence of Joule and Thomson heating which are generated concomitantly during the high current flow along the p–n legs. Thermal contact of the cold substrate with the cold end (load) is physically disconnected prior to the arrival of the ''thermal wave-front'', thus maintaining a low temperature on the cold junction of the device. It is highlighted that prior to contact duration, the amount of current supplied to the thermoelectrics produces no cooling effect and correspondingly the temperature achieved at the cold junction is the lowest possible under the ''open'' mode of operation.

2. Energy conservation equation and T–s relation

To evaluate the temperature profile along the thermoelectric arm, one requires the energy conservation equation and it is given by [6]

$$(\rho c_p)\frac{\partial T}{\partial t} = \nabla\cdot(\lambda\nabla T) + \frac{\mathbf{J}^2}{\sigma} \pm \mathbf{J}\Gamma\cdot\nabla T, \tag{1}$$

where $\mathbf{J}$ $(= I/A)$ is the electrical current density, + sign indicates p leg and − sign is valid for n leg of a thermoelectric couple as shown in Fig. 1(c). The third part of right hand side of Eq. (1) corresponds to a heat effect due to the simultaneous presence of an electrical current and a temperature gradient due to Thomson heat effect. The coefficient of Thomson effect is defined as $\Gamma\left(=\frac{\pi}{T}-\frac{\partial\pi}{\partial T}\right)$, where π is the Peltier coefficient as expressed by the product of Seebeck coefficient and temperature, i.e., $\pi = -\alpha T$ (Kelvin relation) [7]. Substituting these relations and using $\nabla\pi = \nabla\pi|_T + \frac{\partial\pi}{\partial T}\cdot\nabla T$, where the first term defines the rise of heat effect in the absence of a temperature gradient [7] into Eq. (1) yields the final energy balance equation as shown below:

$$(\rho c_p)\frac{\partial T}{\partial t} = \nabla\cdot(\lambda\nabla T) + \frac{\mathbf{J}^2}{\sigma} \pm \left[T\mathbf{J}\cdot\nabla\alpha|_T - T\left(\frac{\partial\alpha}{\partial T}\right)\mathbf{J}\cdot\nabla T\right]. \tag{2}$$

Invoking the definition of enthalpy $h(T,p)$ as a function of pressure (p) and temperature

$$h = u + pv,$$
$$\frac{\partial h}{\partial t} = \frac{\partial u}{\partial t} + \frac{\partial(pv)}{\partial t} = \frac{\partial u}{\partial t}, \quad \text{and}$$
$$\frac{\partial h}{\partial t} = \left(\frac{\partial h}{\partial T}\right)_p\frac{\partial T}{\partial t} + \left(\frac{\partial h}{\partial p}\right)_T\frac{\partial p}{\partial t} = c_p\frac{\partial T}{\partial t},$$

where the pressure gradient term is zero. Eq. (1) is now written as

$$\frac{\partial(\rho u)}{\partial t} = \nabla\cdot(\lambda\nabla T) + \frac{\mathbf{J}^2}{\sigma} \pm \mathbf{J}\left(\frac{\pi}{T} - \frac{\partial\pi}{\partial T}\right)\cdot\nabla T. \tag{3}$$

Following the Gibbs law and an energy conservation (Eq. (3)) within a control volume, the basic entropy balance equation can be expressed as

$$\begin{aligned}\frac{\partial(\rho s)}{\partial t} &= \frac{\nabla\cdot(\lambda\nabla T)}{T} + \frac{1}{T}\frac{\mathbf{J}^2}{\sigma} \pm \frac{\mathbf{J}}{T}\left(\frac{\pi}{T} - \frac{\partial\pi}{\partial T}\right)\cdot\nabla T\\ &= \nabla\cdot\left(\frac{\lambda\nabla T}{T}\right) - \lambda\nabla T\cdot\nabla\left(\frac{1}{T}\right)\\ &\quad + \frac{\mathbf{J}^2}{T\sigma} \pm \nabla\cdot\left(\frac{\pi\mathbf{J}}{T}\right) \pm \frac{\mathbf{J}}{T}\cdot\nabla\pi\Big|_T\\ &= \nabla\cdot\left(\frac{\lambda\nabla T}{T} \pm \frac{\pi\mathbf{J}}{T}\right) - \lambda\nabla T\cdot\nabla\left(\frac{1}{T}\right) + \frac{\mathbf{J}^2}{T\sigma} \pm \frac{\mathbf{J}}{T}\cdot\nabla\pi\Big|_T\\ \frac{\partial(\rho s)}{\partial t} &= \nabla\cdot\left(\frac{\lambda\nabla T}{T} \pm \alpha\mathbf{J}\right) + \left[\frac{\mathbf{J}^2}{T\sigma} - \lambda\nabla T\cdot\nabla\left(\frac{1}{T}\right) \pm \mathbf{J}\cdot\nabla\alpha\Big|_T\right],\end{aligned} \tag{4}$$

where the first terms indicate the entropy flux $\mathbf{J}_S$ (W/m^2 K) and the second terms are entropy generation $\mathbf{S}_{gen}$ (W/m^3 K) and these are expressed as

$$\mathbf{J}_S = \frac{\lambda\nabla T}{T} \pm \alpha\mathbf{J}, \tag{5}$$

and

$$\mathbf{S}_{gen} = \overbrace{\frac{\mathbf{J}^2}{T\sigma}}^{\text{Joule effect}} - \overbrace{\lambda\nabla T\cdot\nabla\left(\frac{1}{T}\right)}^{\text{Internal heat loss}} \pm \overbrace{\mathbf{J}\cdot\nabla\alpha|_T}^{\text{Dissipation due to Thomson}}. \tag{6}$$

Eq. (6) refers to the area under the process paths given in a T–s diagram, i.e., energy dissipation between the actual and the ideal cycles, operating over the same hot and cold reservoirs.

With the boundary conditions indicated in Fig. 1(c), for thermoelectric legs of length L ($0 \leqslant x \leqslant L$), the one-dimensional equation for p and n legs become

$$(\rho c_p)\frac{\partial T(x,t)}{\partial t} = \lambda\frac{\partial^2 T(x,t)}{\partial x^2} + \frac{\mathbf{J}^2}{\sigma} \pm \left[T(x,t)\mathbf{J}\cdot\frac{\partial\alpha}{\partial x} - T(x,t)\left(\frac{\partial\alpha}{\partial T}\right)\mathbf{J}\cdot\frac{\partial T(x,t)}{\partial x}\right]. \tag{7}$$

The one-dimensional equations for entropy flux densities on the p leg and n leg are

$$\mathbf{J}_{S,p}(x,t) = \frac{\lambda}{T}\frac{\partial T(x,t)}{\partial x} + \alpha\mathbf{J}, \tag{8}$$

$$\mathbf{J}_{S,n}(x,t) = \frac{\lambda}{T}\frac{\partial T(x,t)}{\partial x} - \alpha\mathbf{J}. \tag{9}$$

Hence, Eqs. (7)–(9) form the necessary equation set for the temperature–entropy diagram. To solve these equations, two boundary conditions are introduced for the non-contact and the contact periods to simulate the operation of the pulsed thermoelectric cooler. During the open-contact operation, only Peltier cooling exists at the cold junction (cj), i.e.,

$$\left.\frac{\partial T}{\partial x}\right|_{x=0} = \frac{\alpha\mathbf{J}T_{cj}}{\lambda}. \tag{10}$$

At hot junction (hj), it is represented by an isothermal heat reservoir, $T|_{x=L} = T_{hj}$. However, during the pulsed or close-contact operation, heat from the cold reservoir or load is transferred to the cold junction and the boundary conditions become

$$\left.\frac{\partial T}{\partial x}\right|_{x=0} = \frac{\alpha\mathbf{J}T_{cj}}{\lambda} + \frac{\dot{q}_{subs}}{\lambda}, \tag{11}$$

where $\dot{q}_{subs}$ is the instantaneous cooling load of the cold substrate.

3. Results and discussion

Fig. 2 shows the transient behaviour of the pulsed thermoelectric cooler where the hot junction is assumed to be constant at $T_{hj} = 308$ K. Based on the physical properties of a thermoelectric cooler, as tabulated in Table 1, the

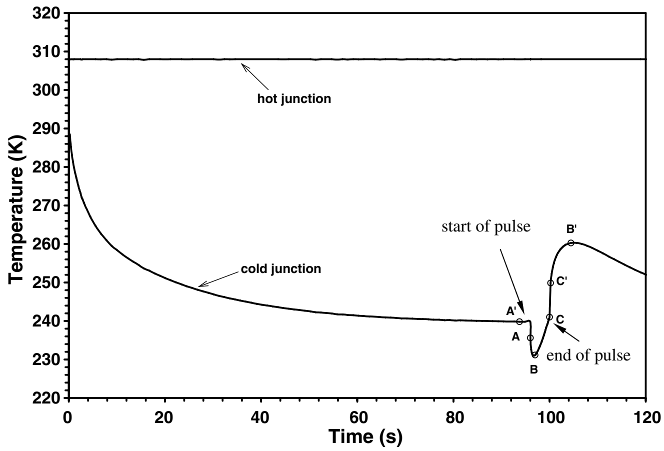

Fig. 2. The transient temperature-time trace of cold reservoir temperature of a pulsed thermoelectric cooler. Point "A" indicates the beginning of pulse period, "B" denotes the lowest temperature reached by the cooler and "C" represents the end of pulse period, "C′" shows the beginning of non-contact period, "B′" indicates maximum temperature rise due to energy balance between the residual heat from the pulsed period and the steady state cooling.

Table 1
Physical parameters of a pulsed thermoelectric cooler (Bi_2Te_3)

Property	Value
Hot reservoir temperature, T_{hj} (K)	308
Thermoelectric element length, L_{te} (mm)	5.8[a]
Cross-sectional area, A_{te} (mm^2)	1[a]
Geometric factor, GF_{te} (mm)	0.1724[a]
Current, I (A)	0.675[a]
Electrical resistivity (ohm cm)	$\rho_0 = 5112.0$, $\rho_1 = 163.4$,
$\rho = (\rho_0 + \rho_1 T_{ave} + \rho_2 T_{ave}^2) \times 10^{-8}$	$\rho_2 = 0.6279$[b]
Seebeck coefficient (V/K)	$\alpha_0 = 210 \times 10^{-6}$,
$\alpha = \alpha_0 + \mu \ln(T/T_0)$	$\mu = 120 \times 10^{-6}$, $T_0 = 300$ K[c]
Thermal conductivity (W/cm K)	$\lambda_0 = 62605.0$,
$\lambda = (\lambda_0 + \lambda_1 T_{ave} + \lambda_2 T_{ave}^2) \times 10^{-9}$	$\lambda_1 = -277.7$, $\lambda_2 = 0.4131$[b]

$T_{ave} = (T_{hj} + T_{cj})/2$.
[a] Remarks Ref. [4].
[b] Remarks Melcor thermoelectric catalogue, MELCOR CORPORATION, 1040 Spruce Street, Trenton, NJ 08648, USA. Web site: www.melcor.com.
[c] Remarks Ref. [8].

simulations with an initial current density of $\mathbf{J}_{np} = 0.675$ A/mm^2 yield an exponential decrease of the cold junction temperature to $T_{c,A'} = 240$ K (denoted by point A′), and beyond which a pulsed current density of $\mathbf{J}_p = 2.025$ A/mm^2 for a duration of 4 s is applied for the pulsed or contact mode. The high pulsed current in the thermoelectrics produces instantaneous Peltier cooling, as shown by the decrease in the cold junction temperature to point B. Concomitantly, the pulsed current generates the Joule and Thomson heating within the p–n legs and this is reflected by the rise of cold junction temperature from point B to C. As no cooling could be achieved by the cold substrate, the cold junction breaks contact with it at point C.

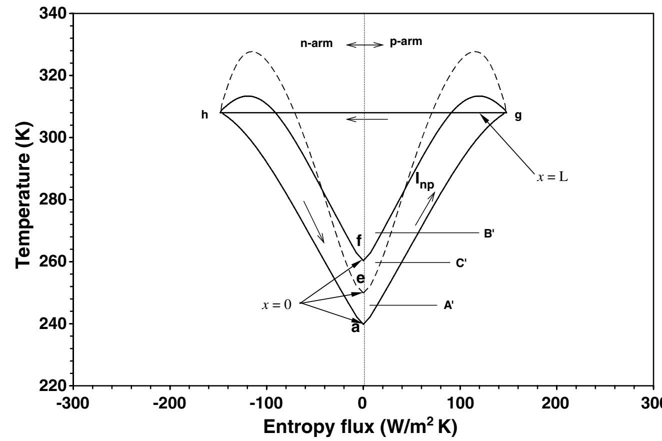

Fig. 3. Temperature–entropy flux (T–s) diagram showing the anti-clockwise loop of a pulsed thermoelectric cooler for the non-pulse duration for three operation points.

However, the residual heat transfer from the mentioned effects is generally a slower phenomenon as compared to Peltier cooling, the temperature of the cold junction continues to rise until the cooling by $\mathbf{J}_{np}$ overcomes the residual heat within the legs, culminating in a maxima for the temperature of the cold junction, as depicted by point B′.

For the non-contact duration, the energy flows in the thermoelectric device can best be followed by tracking the temperature versus entropy fluxes along the p leg in a anti-clockwise direction, i.e., points "a"–"g" of Fig. 3: Point "a" denotes the cold junction temperature and the entropy flux here is taken to be zero or the datum. As holes migrates along the p leg, both entropy flux and temperature increase with the spatial length until point "g" is reached, due primarily to the property changes with the local temperature of Bi_2Te_3 materials such as the electrical resistivity (ohm cm), Seebeck coefficient (V/K) and thermal conductivity (W/cm K). For the given configuration and current density, the maximum entropy flux is about 300 W/m^2 K. At the hot junction which is assumed to remain constant at T_{hj}, the sign of the entropy flux changes from positive to negative due to negative temperature gradient along the n leg, resulting in the isotherm "g"–"h" line on the T–s diagram. Following the path in an anti-clockwise direction, the local entropy flux increases from point "h" to point "a", completing the cycle (denoted by A′) on the T–s diagram.

Two other process cycles could also be observed for the non-contact duration, namely cycles "B′" and "C′": Both cycles are subjected to $\mathbf{J}_{np}$ and they show the presence of residual Joulean and Thomson heat within the p–n legs of the thermoelectrics. The balance between the cooling rate generated by the $\mathbf{J}_{np}$ and the amount of residual Joule and Thomson heat from the previous pulsed injection yield a local thermal wave front in each of the legs (at distances closer to the hot junction) where the maximum local temperature is higher than that of the T_{hj}.

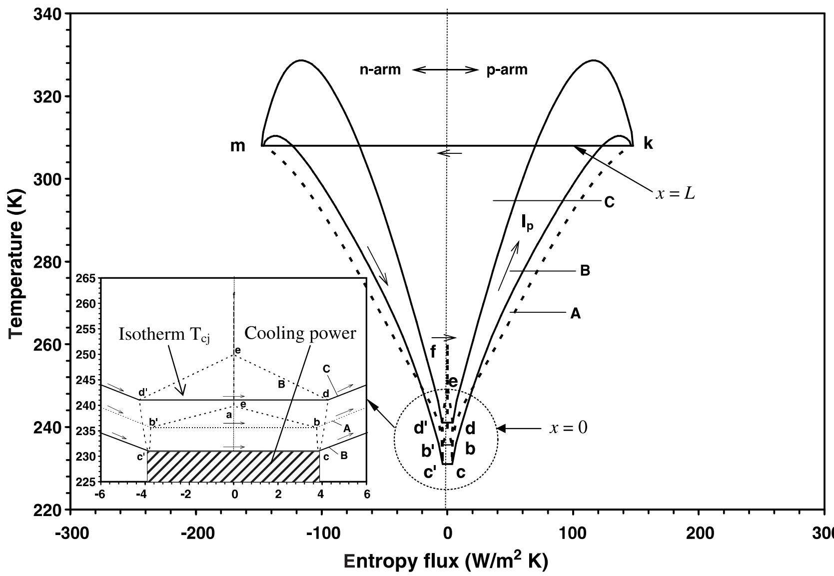

Fig. 4. Temperature–entropy flux (T–s) diagram showing the energy flow details of a pulsed period of thermoelectric cooler. Cycles A–C refer to the beginning of cooling, the lowest temperature reached and the maximum cooling power by the cooler. The details of the processes within the cold junction of thermoelectrics are shown by the small insert, denoted correspondingly by "a"–"c". The enclosed area below T_c isotherms in the T–s diagram indicates the cooling power.

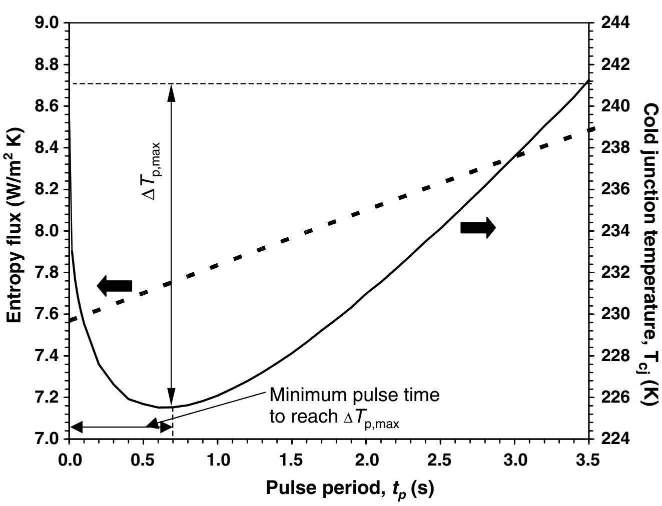

Fig. 5. The effects of pulse periods on entropy flux and the cold junction temperature subjected to a step current pulse of magnitude $M = 4$.

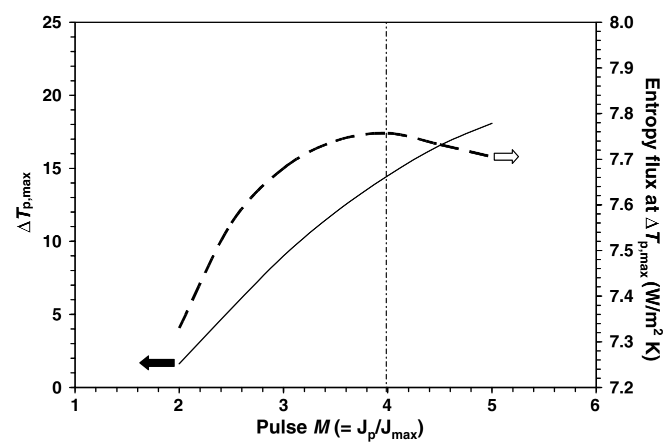

Fig. 6. Maximum pulse cooling difference in temperatures and entropy fluxes as a function of pulse factor, exhibits the optimization.

During closed contact operation, as shown in Fig. 4, point A indicates the commencement of contact interval where the imposed current pulse ($\mathbf{J}_p$) generates a substantial cooling, depressing the cold junction and the cold template temperature from "f" to "a" (see the smaller insert). As opposed to the non-contact duration, the cold junction on the T–s plot has an isotherm path, and the area enclosed below the isotherm b–b′ indicates the amount of cooling produced at point A of the contact operation. Similar isotherms c–c′ and d–d′ correspond to the points B and C during the transients. Although the enclosed area for point C is slightly larger than that of point B, but the cold junction temperature of point C is found to be higher, caused by the diffusion of Joule heat from the legs of the thermoelectrics.

No cooling power is developed during non-contact period but the cooling power is generated during pulse period. Fig. 5 shows the time evolution of entropy flow and temperature at the cold junction and calculates the minimum time to reach the maximum temperature difference between the super-cooling and the steady state or $\Delta T_{p,max}$. The characteristics time, entropy flux and cold end temperature as shown in Fig. 5 may be used to characterize the pulse cooler as functions of length of pulse t_p, pulse factor M, and pulse current density, J_p. This graph is helpful to design a cooler where the user would easily calculate the amount of increasing cooling, cooling behaviours, the needed pulse current and the time between pulses.

The effects of pulse factors on entropy flux at cold end and the maximum temperature drop or $\Delta T_{p,max}$ are shown in Fig. 6 and the optimization is obtained at pulse factor 4.

4. Conclusions

The authors have successfully plotted the *T–s* diagrams for the transient features of a pulsed thermoelectric cooler. The thermodynamic formulation (based on the Gibbs law) provides the necessary expression for the entropy flux that is expressed in terms of the basic variables describing the device, namely, the current density, Seebeck coefficient, the local temperature and temperature gradient. Using the *T–s* diagram, the process paths of the pulsed and non-pulsed operations of thermoelectric cooler are accurately mapped and it has immense pedagogical value for cycle evaluation, depicting the useful energy flows and "bottlenecks" of cycle operation.

References

[1] L.S. Stil'bans, N.A. Fedorovitch, Cooling of thermoelectric cells under nonstationary conditions, Sov. Phys. Tech. Phys. 3 (1958) 460–463.
[2] K. Landecker, A.W. Findlay, Study of the fast transient behaviour of Peltier junctions, Solid State Electron. 3 (1961) 239–260.
[3] R.L. Field, H.A. Blum, Fast transient behavior of thermoelectric coolers with high current pulse and finite cold junction, Energy Conv. 19 (3) (1979) 159–165.
[4] G.J. Snyder, J.P. Fleurial, T. Caillat, R. Yang, G. Chen, Super-cooling of Peltier cooler using a current pulse, J. Appl. Phys. 92 (3) (2002) 1564–1569.
[5] H.T. Chua, K.C. Ng, X.C. Xuan, C. Yap, Temperature entropy formulation of thermoelectric thermodynamic cycles, Phys. Rev. E 65 (2002) 056111-1–056111-6.
[6] D.M. Rowe (Ed.), CRC Handbook of Thermoelectrics, CRC Press, Boca Raton FL, 1995.
[7] S.R. De Groot, P. Mazur, Non-equilibrium Thermodynamics, North-Holland Pub Co, Amsterdam, 1962.
[8] W. Seifert, M. Ueltzen, E. Muller, One-dimensional modelling of thermoelectric cooling, Phys. Stat. Sol. (a) 194 (1) (2002) 277–290.